Revista Mexicana de Física **36** *No. 2(1990) 220–230*

Neutron emission in light heavy ion reactions

M.E. Ortiz, A. Dacal, F.M. Lugo

Instituto de Física, Universidad Nacional Autónoma de México,
Apartado postal 20-364, 01000 México, D.F.

J. Gómez del Campo

Oak Ridge National Laboratory,
Oak Ridge, TN 37831, USA

(Recibido el 16 de noviembre de 1989; aceptado el 25 de enero de 1990)

Abstract. Neutron emission cross sections were measured for several light heavy-ion systems, using a 4π detector. The systems studied were $^{12}C + ^{12}C$, $^{12}C + ^{13}C$, $^{13}C + ^{13}C$, $^{14}N + ^{12}C$, $^{16}O + ^{12}C$ and $^{16}O + ^{16}O$ at bombarding energies around the Coulomb barrier. A detail Hauser-Feshbach analysis was done and good agreement with the data was found. The $^{12}C + ^{12}C$ system shows a great deal of resonances which are correlated to other channels. Fewer resonance are seen for the $^{12}C + ^{13}C$ and $^{12}C + ^{16}O$ systems.

PACS: 25.70.Gh

1. Introduction

The discovery of resonances in the $^{12}C + ^{12}C$ systems, correlated to many decay channels [1], initiated a great deal of experimental activity in the past two decades. A recent review on this subject is given by T. Cormier [2]. One of the motivations of the present measurements was to search for resonance structures in light heavy-ion systems by measuring the total angle integrated neutron yields. This technique should reveal most of the resonance structure since statistical fluctuations, which commonly confuse the resonance behavior, are severely damped out due to the many channels included in the total yield measurements. In addition, very little information is available on neutron decay for these systems up to date.

Another important motivation for this measurements consists in the study of the gross energy dependence of the reaction mechanisms responsible for the neutron emission. We have concentrated the measurements for bombarding energies covering about 50% below and above the Coulomb barrier in the region which is relevant for extrapolation to energies of astrophysical interest.

Although the bombarding energies used in the present measurements are low, the excitation energies are so high that not only the one neutron emission channel is important but also multiparticle — (mostly p's and α's) neutron channels are open and need to be included in the calculations. To this effect the code LILITA has been used, but improved in many aspects dealing with the entrance channel

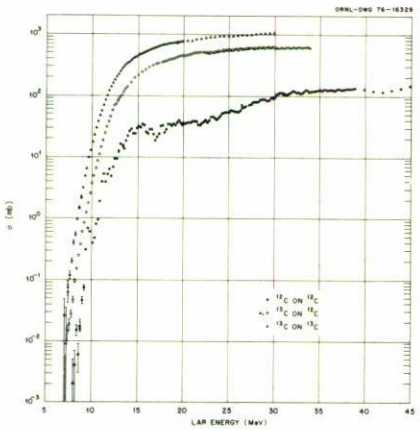

FIGURE 1. Neutron emission cross sections measured for different combinations of carbon isotopes.

spin distribution, optical model transmission coefficients, and use known discrete states of residual nuclei wherever it's possible. In Sec. 2 we discuss the experimental details and Sec. 3 is dedicated to the study of the resonance behavior. Sec. 4 shows the experimental data on the gross energy dependence. Conclusions are presented in the last section.

2. Experimental procedure

The present measurements were performed using beams of ^{12}C, ^{14}N and ^{16}O extracted from the ORNL EN Tandem Accelerator. The 4π neutron measurements were done with the graphite sphere neutron detector described in Ref. [3]. The carbon targets employed were of natural isotopic composition and of enriched $^{13}C(99\%)$. They were evaporated into thick tantalum disc that stopped the beam. The target were placed at the end of the vacuum beam pipe which was introduced in the center of the graphite sphere through a 10 cm quadrangular opening. The target assembly was electrically isolated and was used as a Faraday cup to measure the integrated charge. For the $^{12}C + {}^{12}C$ measurements a thin target of $7\mu g/cm^2$ was used to reduce as much as possible the energy average of the resonant structure. For the measurements on the ^{16}O an implanted target was prepared, implanting the ^{16}O ions at 100 keV. Typical target thickness were all around 20 to $30\mu g/cm^2$. After a series of measurements the target was removed and replaced by a blank tantalum disc which was used to measure the neutron background coming from reactions on the tantalum. Typical neutron production cross sections were a factor of 100 down respect to the ones with the real targets. Room background was also estimated by counting several hours before and after a major run. The over all accuracy of the measurements is $\pm 7\%$ and is given mostly by target thickness uncertainties and

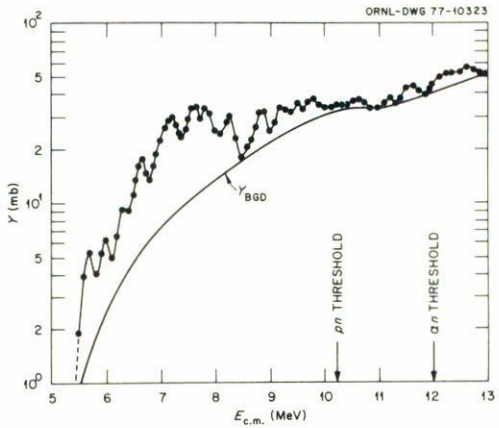

FIGURE 2. $^{12}C + ^{12}C$ neutron emission cross sections as a function of center of mass energy. The solid curve represents an empirical estimation of a non resonant background, as explained in the text.

current integration. Background and counting statistics alone were below 3%. Fig. 1 shows the typical results obtained for the total neutron emission. As can be seen the cross sections can be measured over several orders of magnitude. The data shown in Fig. 1 corresponds to combinations of different carbon isotopes.

3. Experimental results on resonant structure

From all the systems studied the $^{12}C+^{12}C$ is by far the richest in resonant structure. Fig. 2 shows the yield in mb of neutron emission *vs* the center of mass energy (E_{cm}) in the range of 5 to 13 MeV. As can be seen, the resonant structure is evident. To analyze in more detail this structure a nonresonant cross section (Y_{BGD}) is defined in Fig. 2 and then subtracted from the data. The Y_{BGD} curve is an empirical estimation of the non resonant background including an additional constraint of a smooth energy dependence consistent with a Hauser-Feshbach calculation, and normalized to the minimum that can be resolved in the experimental excitation function. Other technics, such as running averages, used in Ericson fluctuation analyses gave non smooth backgrounds. Improvement in this analysis can be done only through a significant reduction of the experimental energy resolution.

The result Y–Y_{BGD} is shown in Fig. 3. The vertical arrows drawn in the figure indicate the energy for which previous resonances have been reported [2,4–6] for various exit channels (n, p, α and ^{8}Be). Some of the spin suggestions are also given. The first important comment to make about the data of Fig. 3 is to determine whether or not the structure seen can be account for in the normal frame work of Ericson fluctuations, as has been discussed in several heavy-ion excitation function

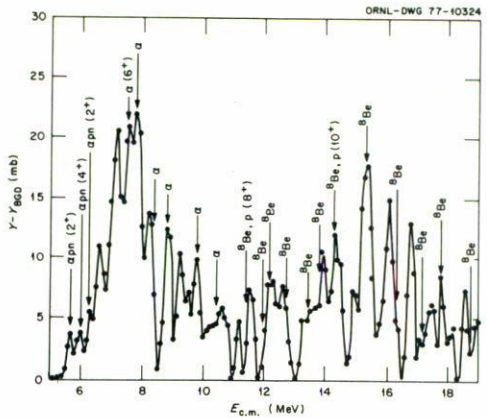

FIGURE 3. Resonant structure observed for $^{12}C+^{12}C$ system. The yield is defined as the subtraction of the estimated background given on Fig. 2, from the measured cross sections. The arrows point to the energies where previous resonances have been reported.

measurements [7,8]. For the $^{12}C + ^{12}C$ reaction at $E_{cm} = 7.5$ MeV we calculated, using the code STATIS [9], that the number of effective channels N_{eff} is about 48. The corresponding probability distribution for the ratio of a given cross section divided by the average, as given for example in Ref. [7], will indicate that most of the fluctuations should be below 10% of the average cross section. This is too small to account for the data of Fig. 3. Another important non statistical effect is that many of the structure seen in Fig. 3 are correlated to other exit channels. From the data presented on Fig. 3 one has to conclude that essentially all the structure is related to real resonances in the $^{12}C + ^{12}C$ system.

The system $^{12}C+^{16}O$ has not been studied as much as the $^{12}C+^{12}C$, nevertheless in the present measurements some structure can be seen also in the energy range of 7 to 10 MeV. Fig. 4 shows the excitation function of the neutron yield for this system and as we see, two clear resonances are observed at 7.71 and 8.5 MeV. For this case the number of effective channels is about 120, and no fluctuations should be seen. One way to remove the strong energy dependence of the cross section, and to enhance the resonant behavior, is to plot the Σ factor which is proportional to the nuclear S factor [10]. This is done for the data of Fig. 4 and is presented in Fig. 5. The resonances at 7.7, 8.5 and 9.2 are evident. Broader and weaker resonances can also be observed at higher energies. To the best of our knowledge this is the first time that this subcoulomb resonances have been reported for the $^{12}C + ^{16}O$ system.

The system $^{13}C+^{12}C$ has been studied with some detail and conflicting evidence has been reported concerning the statistical *vs* resonances behavior [11,12]. In Fig. 6, we show our $^{12}C + ^{13}C$ neutron emission data for the center of mass energy range of 6 to 12 MeV. As follows from the figure, weak resonances are seen at about 9.2 and 10.3 MeV. The arrows drawn in the figure correspond to anomalies reported

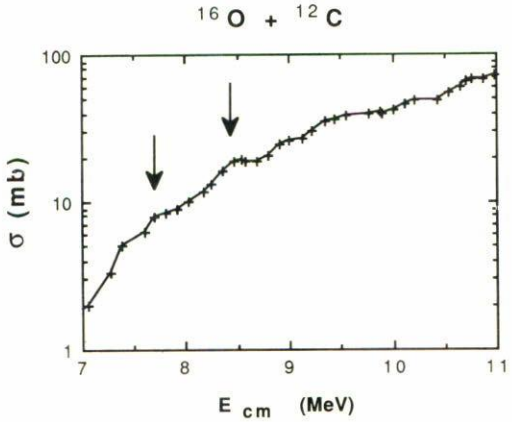

FIGURE 4. Neutron emission cross sections for the $^{12}C+^{16}O$ systems. The arrows show resonances observed at 7.7 and 8.5 MeV.

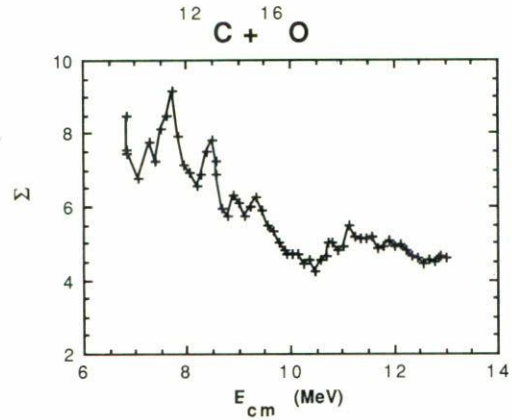

FIGURE 5. The Σ factor (proportional to the nuclear S factor) for the $^{12}C + ^{16}O$ systems. This plot enhances the resonant structure discussed in Fig. 4.

for the α [11], γ [12], and elastic [11,12] yields. Due to the fact that for this reaction the number of effective channels is extremely large ($N_{\text{eff}} = 5000$) no fluctuations are possible and all the structures should be considered as resonaces. This data were taken with a ^{13}C beam on a ^{12}C target and therefore no contamination of the $^{12}C + ^{12}C$ reaction is possible. No other of the systems studied shows convincing evidence of resonances and we concluded that they should be peculiar of alpha-like systems.

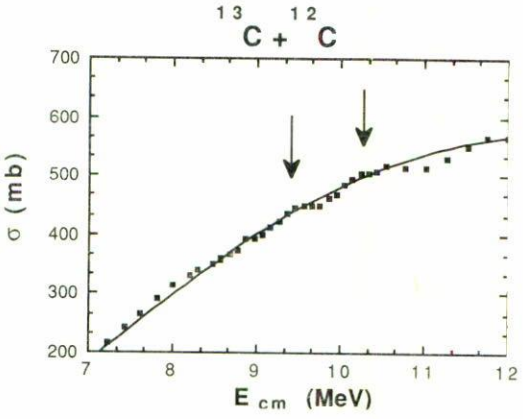

FIGURE 6. Neutron yield excitation function measured for the $^{12}C + ^{13}C$ system. The arrows indicate resonances previously reported for 9.2 and 10.3 MeV. The smooth solid line is drawn only to guide the eye.

4. Experimental results on gross energy dependence

One convenient way to analyze the gross energy dependence of the total neutron yield, and to remove the strong dependence with energy, is to define the neutron multiplicity as the ratio of $\sigma_n/\sigma_{\text{fus}}$, where σ_n is the measured n yield and σ_{fus} is the experimental fusion cross section. The fusion cross sections used were those reported in the literature. For the $^{12}C + ^{12}C$ the measurements of Ref. [13] were used, and for $^{12}C + ^{13}C$ those of Ref. [14] were used.

Measurements for the $^{12}C + ^{14}N$ systems are reported in Refs. [15,16] and the ones for $^{12}C + ^{16}O$ are in Refs. [14, 17–19]. The fusion cross section values reported in Ref. [13] were used for $^{16}O + ^{16}O$ measurements. The experimental ratios on neutron multiplicities (open points) are given in Figs. 7 through 10. From the data given in these figures, the relative importance of the neutron channels can be assessed. For example, for the $^{12}C + ^{12}C$ systems (Fig. 7) neutron emission accounts for about 10 to 20% of the fusion cross section, however for the $^{12}C + ^{13}C$ (Fig. 8) is almost 80%. Of course, these differences reflect just the number of neutron channels available for these two systems.

Detail theoretical calculations of the neutron multiplicities were done within the frame work of the Hauser-Feshbach model, using the code LILITA [20]. The following modifications were done to the code, so it could be used to calculate the neutron multiplicities for entrance channel bombarding energies close to or below the Coulomb barrier: *i)* To improve the level density at low excitation energies the actual known levels were given for energies up to about 12 MeV. For higher excitation energies the usual level density Fermi gas model was employed with typical level density parameters a, ranging from $A/6$ to $A/7$. For example the a

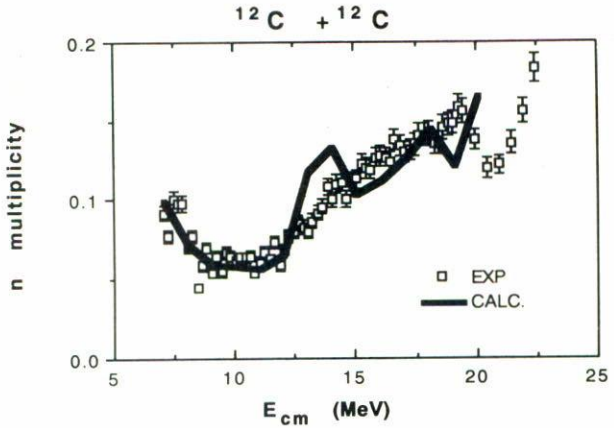

FIGURE 7. Neutron multiplicity as a function of center of mass energy for $^{12}C + ^{12}C$ system. The solid line represents the Hauser-Feshbach calculations.

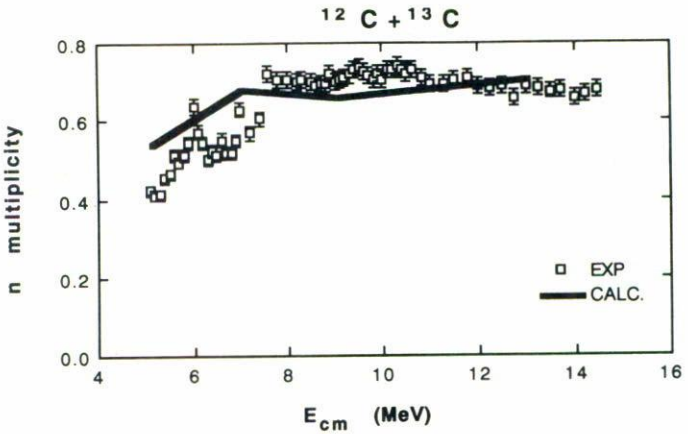

FIGURE 8. Neutron multiplicity as a function of center of mass energy for $^{12}C + ^{13}C$ system. The solid line represents the Hauser-Feshbach calculations.

values for ^{20}Ne, ^{22}Na and ^{24}Mg were 3.4, 2.8, and 3.45 respectively. *ii)* It was also necessary to calculate the transmission coefficients for every exit channel, therefore an optical model routine was incorporated using the code HOP2 [21]. The optical model parameters used for neutrons and protons were those recommended by the Perey and Perey [22] systematics. The set of parameters employed for the alpha channel was: $V = 50$ MeV, $R_V = 1.17 + 1.77/A^{1/3}$ fm, $a_V = 0.576$ fm, $W_I = 1.65(A^{1/2}) - 2$, $R_W = R_V$, $a_W = a_V$ [23]. *iii)* Entrance channel Tl's were also given explicitly. The optical model code PTOLEMY [24] was used for this purpose.

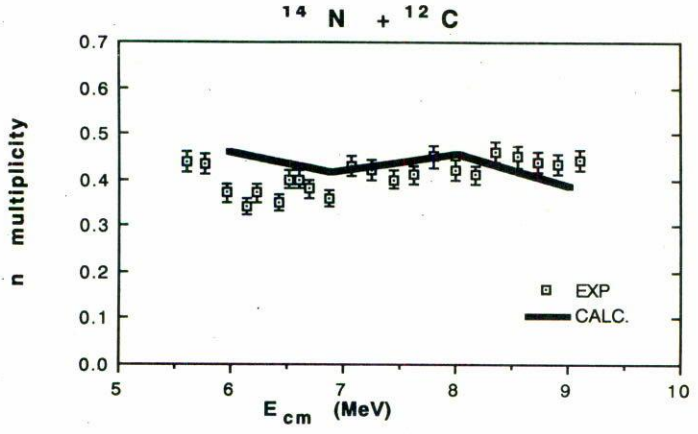

FIGURE 9. Neutron multiplicity as a function of center of mass energy for $^{12}C + ^{14}N$ system. The solid line represents the Hauser–Feshbach calculations.

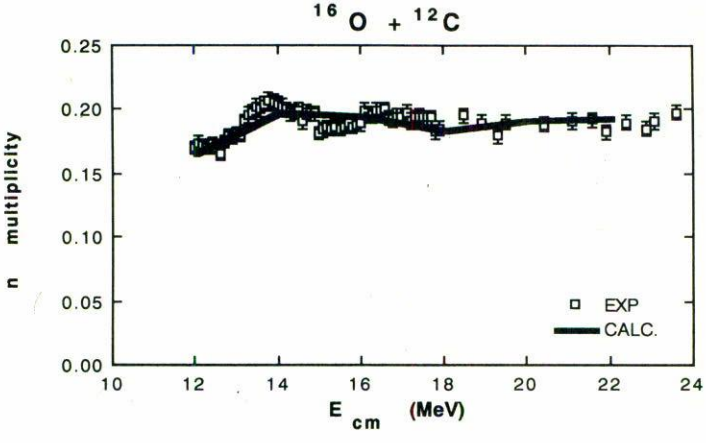

FIGURE 10. Neutron multiplicity as a function of center of mass energy for $^{12}C + ^{16}O$ system. The solid line represents the Hauser-Feshbach calculations.

The election of a good potential, to calculate the entrance channel transmission coefficients was essential to get acceptable fits for each system. We chose potentials that were reported to fit elastic scattering data [25], or fusion cross sections at low energies [26]. For $^{12}C + ^{12}C$, $^{12}C + ^{16}O$ and $^{16}O + ^{16}O$ folding-model potentials derived using Satchler-Love effective force [27] were used together with a Woods-Saxon imaginary potential of energy dependent depth of $-0.5E$ MeV and radius and diffuseness taken from Ref. [28]. A standard optical model calculation recommended in Ref. [29] ($V = 50$ MeV, $R_O = 1.22$ fm, $a = 0.4$ fm) was used for $^{12}C + ^{13}C$

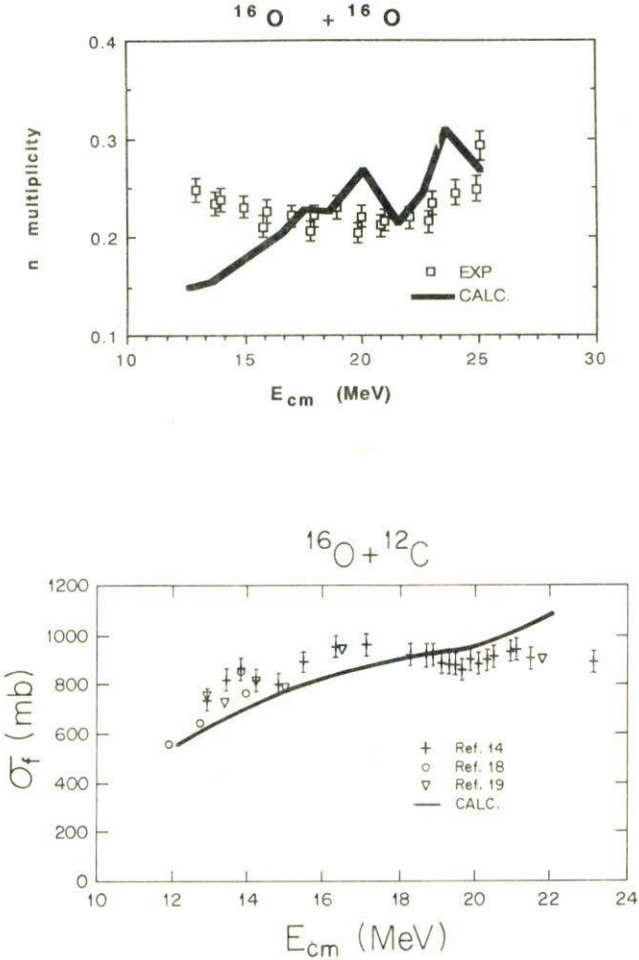

FIGURE 12. Total cross section (mostly fusion) in mb for $^{16}O + ^{12}C$ system. The optical model calculation is represented by the solid line.

and $^{14}N + ^{12}C$ systems. The depth of the imaginary potential was tacken by an extrapolation of the linear energy dependence shown in Fig. 8 of Ref. [30]. Total cross sections within the appropriate energy range for each system were well reproduced by the chosen potentials as can be seen in Fig. 12, where $^{12}C + ^{16}O$ experimental total fusion cross section are plotted together with the result of the calculated ones.

The definition of σ_{fus} used through out the calculations is

$$\sigma_{\text{fus}} = \pi\lambda^2 \sum_J \left[\frac{(2J+1)}{(2i+1)(2I+1)}\right] \sum_{\ell s} (2\ell+1) T\ell,$$

where the total angular momentum J is $J = \ell + s$ with ℓ being the orbital angular momentum and s the channel spin. $s = I + i$ where I is the spin of the target and i that of the projectile.

Fits such as those shown in Fig. 12 were obtained for all the other systems. The results of the neutron multiplicity given by the LILITA calculations using the procedure just described are shown by the solid lines in Figs. 7 to 11. As can be seen from these figures, the general trend of the data is very well reproduced having maximum deviation between theory and experiments of about 60% like for the case of the $^{16}O + {}^{16}O$ system (Fig. 11).

5. Conclusions

The study of neutron emission on light heavy-ion systems gave interesting results on the reaction mechanisms on resonances and compound nucleus formation. The observed resonances on $^{12}C + {}^{12}C$ systems are well correlated with the ones seen previously in other decay channels. Also a couple of resonances are confirmed for the $^{12}C + {}^{13}C$ system. Previously unreported resonances were found for the $^{12}C + {}^{16}O$ system and should be interesting to study the elastic scattering and other reactions channels in order to establish the spin and parities of the resonances. The study on the gross energy dependence of the cross section is well understood by the complete fusion and equilibrium decay mechanism, although it is important to perform the best Hauser-Feshbach calculations possible in order to produce acceptable results.

Acknowledgment

It is a pleasure to acknowledge the calculations and several valuable discussions on the election of the folding potentials to Dr. M.E. Brandan. The research participation of two of us M.E. Ortíz and A. Dacal has being sponsored in part by CONACyT under contract No. PC228CCOX880231. Also M.E. Ortíz acknowledges travel support received by ORNL, Oak Ridge National Laboratory is operated by Martin Marietta Energy Systems, under contract No. DE-AC05-84OR21400 with the U.S. Department of Energy,

References

1. E. Almquist, D.A. Bromley, J.A. Kuehner and B. Whalen, *Phys. Rev.* **130** (1963) 1140.
2. T.M. Cormier, *Ann. Rev. Nucl. Part. Sci.* **32** (1982) 271.
3. R.L. Macklin, *Nucl. Instr. and Meth.* **1** (1957) 335.
4. E.R. Cosman, A. Sperduto, W.H. Moore, T.N. Chin and T.M. Cormier, *Phys. Rev. Lett.* **27** (1971) 1074.

5. D.R. James and N.R. Fletcher, *Phys. Rev.* **C17** (1978) 2248.
6. J.R. Patterson, H. Winkler and C.S. Zaidins, *Astrophys. J.* **157** (1969) 367.
7. J. Gómez del Campo, J.L.C. Ford, R.L. Robinson and P.H. Stelson, *Phys. Rev.* **C9** (1974) 1258.
8. M.E. Ortíz, E. Andrade, M. Cárdenas, A. Dacal, A. Menchaca Rocha, J.L.C. Ford, J. Gómez del Campo, R.L. Robinson, D. Shapira and E. Aguilera, *Phys. Rev.* **C22** (1980) 1104.
9. R.G. Stokstad, Yale University Wright Nuclear Structure Laboratory Report 52 (1972).
10. D.D. Clayton, *Principles of Stellar Evolution and Nucleosynthesis.* McGraw Hill, New York (1968).
11. D.J. Crozier and J.C. Legg, *Phys. Rev. Lett.* **33** (1974) 782.
12. R.A. Dayras, R.G. Stokstad, Z.E. Switkowski and R.M. Wieland, *Nucl. Phys.* **A265** (1976) 153.
13. Q. Haider and F. Barry Malik, *Atomic and Nuclear Data Tables* **31** (1984) 185.
14. D.G. Kovar, D.F. Greesaman, T.H. Braid, Y. Eisen, W. Henning, T.R. Ophel, M. Paul, K.E. Rehm, S.J. Sanders, P. Sperr, J.P. Shiffer, S.L. Tabor, S. Vigdor and Zeidman, *Phys. Rev.* **C20** (1979) 1305.
15. J.A. Kuehner and E. Almquist, *Phys. Rev.* **134** (1964) 1229.
16. J. Gómez del Campo, R.G. Stokstad, J.A. Biggerrstaff, R.A. Dayras, A. Snell and P.H. Stelson, *Phys. Rev.* **C19** (1979) 2170.
17. J.J. Kolata, R.M. Freeman, F. Hass, B. Heusch and A. Gellman, *Phys. Lett* **65B** (1976) 333.
18. Y. Eyal, M. Beckman, R. Chechik, Z. Fraenkel and H. Stocker, *Phys. Rev.* **C13** (1976) 1527.
19. A.D. Frauley, N.R. Fletcher and L.C. Dennis, *Phys. Rev.* **C25** (1982) 860.
20. J. Gómez del Campo and R.G. Stokstad, Oak Ridge Progress Report ORNL/Tm–7295.
21. J. Cramer and Y.D. Chan, *private communication.*
22. C.M. Perey and F.G. Perey, *Atomic and Nuclear Data Tables* **17** (1976) 1.
23. F. Puhlhofer, *Nucl. Phys.* **A280** (1977) 267.
24. M.H. Macfarlane and S.C. Pieper, ANL Report ANL–76–11, (1976).
25. G. Pantis and J.M. Pearson, *Phys. Rev.* **C36** (1987) 1408.
26. R.G. Stokstad, Proceedings of the Topical Conference on Heavy Ion Collisions, Fall Creek Falls, Tennessee (1977).
27. G.R. Satchler and W.G. Love, *Phys. Rep.* **55** (1979) 183.
28. Q. Haider and B. Cuyec, *Nucl. Phys.* **A429** (1984) 116.
29. R.G. Stokstad, Z.E. Switkowski, R.A. Dayras and R.W. Wieland, *Phys. Rev. Lett.* **37** (1976) 888.
30. R.G. Stokstad, R.M. Wieland, R.G. Satchler, C.B. Fulmer, D.C. Hensley, S. Raman, L.D. Rickertsen, A.H. Snell and P.H. Stelson, *Phys. Rev.* **C20** (1979) 655.

Resumen. Se midieron secciones de emisión de neutrones para diferentes sistemas de iones pesados usando un detector 4π. Los sistemas estudiados fueron $^{12}C+^{12}C$, $^{12}C+^{13}C$, $^{13}C+^{13}C$, $^{14}N+^{12}C$, $^{16}O+^{12}C$ y $^{16}O+^{16}O$ a energías de bombardeo alrededor de la barrera Coulombiana. Se llevó a cabo un análisis de Hauser-Feshbach detallado obteniéndose un buen acuerdo con los datos. El sistema $^{12}C+^{12}C$ muestra un cierto número de resonancias correlacionadas a otros canales de evaporación. También se observaron resonancias, aunque más escasas, en los sistemas $^{12}C+^{13}C$ y $^{12}C+^{16}O$.